MODELLING OF CRACK PROPAGATION THROUGH FRAGMENTED SOLIDS

A.N. Galybin and A.V. Dyskin
School of Civil and Resource Engineering, The University of Western Australia, Australia

ABSTRACT

The paper discusses crack propagation in what we call fragmented solids, i.e. either fully discontinuous or heavily cracked materials. The propagating cracks follow ruptured paths caused by offsets on the interfaces. This situation is modelled as a propagation of cracks in plane elastic bodies with two mutually orthogonal sets of pre-exiting weak interfaces. It is assumed that crack follows the horizontal interfaces, while the vertical ones arrest the crack and produce offsets in the crack path. The method of singular integral equations and the Gauss-Chebyshev quadrature for singular integrals is used with a modification that preserves positions of collocations on every crack segment when crack propagates. The stress intensity factors (SIFs) are calculated for different crack trajectories. Based on these calculations it is found that the preferable crack trajectories are oblique rather than horizontal as would be expected due to symmetry. One can call this phenomenon the symmetry breaking. The exponent of the power law describing the increase of the mode I SIF with the increasing crack length is close to 0.4 as opposite to 1/2 for the conventional crack.

1 INTRODUCTION

Conventional Fracture Mechanics deals with continuous (at the scale of interest) solids in investigation of the mechanisms of their failure, in particular, various aspects of propagation of one or, sometimes, several cracks. However, the class of continuous materials is not the only one existing in nature or even in engineering: fragmented solids and heavily cracked materials (with multiple cracks commensurate with the scale of interest) are not less common than the continuous ones. Important natural examples are the blocky and heavily fractured rock masses the resource industry often has to deal with and fractured ice (the Earth ice covers are not the only ones of interest, the fractured ice on the Jupiter moon Europa has recently attracted considerable interest, e.g., Hoppa et al. [1]). Engineering examples are represented by fractured but still stable coatings (interesting, for instance, from the point of view of their durability against impacts) and mortar-free structures in Civil Engineering, from ancient structures (pyramids, dry stone walls) to modern structures based on interlocking bricks (e.g. Dyskin et al. [2]).

From the point of view of crack propagation both fragmented solids, i.e. fully discontinuous materials and heavily cracked materials can be treated similarly, since they provide multiple interfaces intersecting the path the crack would take in a continuous material and produce ruptured trajectories. For that reasons we will refer to both types of materials as to *fragmented solids*.

The present study considers ruptured crack paths caused by offsets on the interfaces in a 2D body. It is assumed that the latter are composed of two mutually orthogonal sets of parallel segments as shown in Figure 1. The initial crack is straight and oriented perpendicular to the remote tensile load (that assumed to be insufficient to open the interfaces).

The crack is assumed to propagate along the horizontal interfaces with vertical interfaced producing offsets in the crack trajectories as shown in Figure 1. This view on crack propagation corresponds to the so-called “compressional crossing”, a phenomenon experimentally observed by Renshaw and Pollard [3] and also in FEM simulations (McConaughy and Engelder [4]).

2 MODEL OF PROPAGATION OF CRACK WITH RUPTURED TRAJECTORY

The following singular integral equation (SIE) and condition of single valuedness of displacements (that ensures uniqueness of solution of the SIE) describe equilibrium of a plane with an arbitrary curvilinear crack (Savruk [5])

$$\frac{1}{2\pi}\int_{\Gamma}\left\{\left[\frac{2}{t-t'}+k_1(t,t')\right]Q(t)\,dt+k_2(t,t')\overline{Q(t)\,dt}\right\}=\sigma(t')+i\,\tau(t'),\quad t'\in\Gamma,\ \int_{\Gamma}Q(t)\,dt=0 \quad (1)$$

Here $Q(t)=\frac{2G}{1+\kappa}\frac{d}{dt}\left[\left(v^{+}(t)-iu^{+}(t)\right)-\left(v^{-}(t)-iu^{-}(t)\right)\right]$ is normalised density of the displacement discontinuity across the crack (unbounded at its ends), $\sigma(t')+i\tau(t')$ is stress vector applied to the crack surfaces, t and t' are points on the crack contour, Γ, in complex plane, and regular kernels are

$$k_1(t,t')=\frac{d}{dt'}\ln\frac{t-t'}{\bar{t}-\bar{t}'},\quad k_2(t,t')=-\frac{d}{dt'}\frac{t-t'}{\bar{t}-\bar{t}'} \quad (2)$$

For a polygonal contour Γ composed of N straight connected segments, Γ_k. ($k=1...N$) each segment being characterised by a complex coordinate of its centre, χ_k, its half-length L_k, and the angle of inclination, θ_k, to the positive direction of the x-axis:

$$\Gamma=\bigcup_{k=1}^{N}\Gamma_k,\quad \Gamma_k=\left\{t_k:\ \ t_k(\eta)=L_k e^{i\theta_k}\eta+\chi_k,\quad |\eta|\le 1\right\} \quad (3)$$

By introducing unknown functions $Q_k(\eta)=Q(t_k(\eta))$ on each segment one can rewrite (1) as

$$\sum_{k=1}^{N}\frac{L_k}{2\pi}\int_{-1}^{1}\left\{\left[\frac{2}{t_k(\eta)-t'}+k_1(t_k(\eta),t')\right]e^{i\theta_k}Q_k(\eta)+k_1(t_k(\eta),t')e^{-i\theta_k}\overline{Q_k(\eta)}\right\}d\eta=\sigma(t')+i\,\tau(t')$$

$$\sum_{k=1}^{N}L_k e^{\theta_k}\int_{-1}^{1}Q_k(\eta)\,d\eta=0 \quad (4)$$

Once a solution of (4) is found one can determine the stress intensity factors, K_I and K_{II}, at the left and right ends from the corresponding asymptotics of $Q_1(\eta)$ at the left end of the first segment and $Q_N(\eta)$ at the right end of the second segment.

Since in general solutions of (1) are unbounded at the ends, solutions of (4) are sought as unbounded for the left end of Γ_1 and the right end of Γ_N the solutions on all other segments being bounded. Therefore the functions $Q_k(\eta)$ can be replaced by new regular functions $q_k(\eta)$ as follows

$$Q_1(\eta)=\sqrt{\frac{1-\eta}{1+\eta}}q_1(\eta),\quad Q_k(\eta)=\sqrt{1-\eta^2}\,q_k(\eta),\quad k=2\ldots N-1,\quad Q_N(\eta)=\sqrt{\frac{1+\eta}{1-\eta}}q_N(\eta) \quad (5)$$

After substitution of (5) into (4) all regular integrals can be calculated in accordance with the following Gauss-Chebyshev quadratures (Erdogan and Gupta [6])

$$\begin{aligned}
&\frac{1}{\pi}\int_{-1}^{1}\frac{(1\pm\xi)q(\xi)}{\sqrt{1-\xi^2}}\,d\xi=\frac{1}{n}\sum_{k=1}^{n}(1\pm\xi_k)q(\xi_k),\quad \xi_k=\cos\frac{2k-1}{2n}\pi,\quad k=1\ldots n\\
&\frac{1}{\pi}\int_{-1}^{1}\sqrt{1-\eta^2}\,q(\eta)\,d\eta=\frac{1}{n}\sum_{j=1}^{n-1}(1-\eta_j^2)q(\eta_j),\quad \eta_j=\cos\frac{j\pi}{n},\quad j=1\ldots n-1
\end{aligned}\tag{6}$$

These formulae are exact if $q(\xi)$ is a polynomial of $(2n\text{-}2)$ degree for the first equation in (6) and of $(2n\text{-}3)$ degree for the second equation.

For singular integrals the Gauss-Chebyshev quadratures have the form

$$\begin{aligned}
&\frac{1}{\pi}\int_{-1}^{1}\frac{1\pm\xi}{\sqrt{1-\xi^2}}\frac{q(\xi)}{\xi-\eta}\,d\xi=\frac{1}{n}\sum_{k=1}^{n}\frac{(1\pm\xi_k)q(\xi_k)}{\xi_k-\eta}+\frac{(1\pm\eta)q(\eta)U_{n-1}(\eta)}{T_n(\eta)}\\
&\frac{1}{\pi}\int_{-1}^{1}\sqrt{1-\eta^2}\,\frac{q(\eta)}{\eta-\xi}\,d\eta=\frac{1}{n}\sum_{j=1}^{n-1}(1-\eta_j^2)\frac{q(\eta_j)}{\eta_j-\xi}-\frac{q(\xi)T_n(\xi)}{U_{n-1}(\xi)}
\end{aligned}\tag{7}$$

Here Chebyshev polynomials

$$T_n(\xi)=\cos(n\arccos\xi),\quad U_{n-1}(\eta)=\sin(n\arccos\eta)\Big/\sqrt{1-\eta^2}\tag{8}$$

have roots ξ_k (k=1…n) and η_j (j=1…n-1) correspondingly as determined in (6). Formulae (7) are exact if $q(\xi)$ is a polynomial of $(2n\text{-}1)$ or $(2n\text{-}2)$ degrees correspondingly.

It is obvious that the terms containing Chebyshev polynomials in (7) vanish at the roots of $U_{n\text{-}1}(\eta)$ and $T_n(\xi)$ correspondingly. Further ξ_k (k=1…n) are used as collocations for the edge segments and η_j (j=1…n-1) are collocations for internal segments. Although quadratures for each segment have been applied separately based on SIE (4), one can now return to the consideration of SIE (1) by introducing the following arrays of nodes, collocations and weights

$$\begin{aligned}
X&=\{t_1(\xi_1),\ldots t_1(\xi_n),t_2(\eta_1)\ldots t_2(\eta_{n-1}),\ldots t_{N-1}(\eta_1),\ldots t_{N-1}(\eta_{n-1}),t_N(\xi_1),\ldots t_{N-1}(\xi_n)\}\\
Y&=\{t_1(\eta_1),\ldots t_1(\eta_{n-1}),t_2(\xi_1)\ldots t_2(\xi_n),\ldots t_{N-1}(\xi_1),\ldots t_{N-1}(\xi_n),t_N(\eta_1),\ldots t_{N-1}(\eta_{n-1})\}\\
W&=\Big\{(1-\xi_1)L_1,\ldots(1-\xi_n)L_1,(1-\xi_1^2)L_2\ldots(1-\xi_{n-1}^2)L_2,\ldots\\
&\qquad\ldots(1-\xi_1^2)L_{N-1},\ldots(1-\xi_{n-1}^2)L_{N-1},(1+\xi_1)L_N,\ldots(1+\xi_n)L_N\Big\}
\end{aligned}\tag{9}$$

The number of nodes and weights is $(n\text{-}1)N$+2, the number of collocation is Nn-2. Discretization of (1) leads to the following system of linear algebraic equations

$$\mathbf{AZ}=\mathbf{B},\quad \mathbf{A}=\begin{pmatrix}\mathbf{K}^{11} & \mathbf{K}^{12}\\ \mathbf{K}^{21} & \mathbf{K}^{22}\\ \mathbf{C} & \mathbf{S}\end{pmatrix},\quad \mathbf{B}=\begin{pmatrix}\boldsymbol{\sigma}\\ \boldsymbol{\tau}\\ \boldsymbol{\delta}\end{pmatrix}\tag{10}$$

Here vector **Z** represent stacked arrays of real and imaginary parts of unknowns $q_k(\eta)$ in (5) at the nodes; the components of matrixes $\mathbf{K}^{pq}$ (((*n*-1)*N*+2)×(*Nn*-2)) (*p, q*=1,2) and vectors **C**, **S**, **σ**, **τ** and **δ** are as follows ($l = 1 \ldots Nn-2, \quad m = 1 \ldots (n-1)N-2$)

$$K_{lm}^{11} = \mathrm{Re}\left(K_{lm}^{1} + K_{lm}^{2}\right), \quad K_{lm}^{12} = \mathrm{Re}\left(-iK_{lm}^{1} + iK_{lm}^{2}\right), \quad K_{lm}^{21} = \mathrm{Im}\left(K_{lm}^{1} + K_{lm}^{2}\right), \quad K_{lm}^{22} = \mathrm{Im}\left(-iK_{lm}^{1} + iK_{lm}^{2}\right)$$
$$\sigma_l = \sigma\left(Y_l\right), \quad \tau_l = \tau\left(Y_l\right), \quad C_m = W_m \cos\left(\theta\left(X_m\right)\right), \quad S_m = W_m \sin\left(\theta\left(X_m\right)\right), \quad \delta_1 = 0, \quad \delta_2 = 0$$
$$K_{lm}^{1} = \frac{W_m}{n} e^{i(\theta(X_m)-\theta(Y_l))} \mathrm{Re}\left(\frac{e^{i\theta(X_m)}}{X_m - Y_l}\right), \quad K_{lm}^{2} = \frac{W_m}{2n} \frac{e^{-i\theta(X_m)}}{\overline{X}_m - \overline{Y}_l}\left(1 - \frac{X_m - Y_l}{\overline{X}_m - \overline{Y}_l} e^{-2i\theta(Y_l)}\right) \tag{11}$$

System (10) is overdetermined if *N*>3, therefore the number of segments in polygonal crack is further assumed to be greater than two. The overdetermined system (11) is solved by the lest squares method

$$\mathbf{Z} = \left(\mathbf{A}^T \mathbf{A}\right)^{-1} \mathbf{A}^T \mathbf{B} \tag{12}$$

The stress intensity factors at the right/left ends (denoted by superscripts "±" respectively) are calculated as follows

$$K_I^- + iK_{II}^- = 2\sqrt{\pi L_1}\ \mathrm{Interp}\left(q_1\left(\xi_j\right), -1\right), \quad K_I^+ + iK_{II}^+ = 2\sqrt{\pi L_N}\ \mathrm{Interp}\left(q_N\left(\xi_j\right), 1\right) \tag{13}$$

where *Interp*(…,…) denotes linear interpolation.

This numerical scheme has been verified against known results for branching cracks It has been found that 4-16 nodes placed on each segment (of equal length) provide the accuracy presented in the handbook by Murakami [7] for different configuration in which the length of the branch and its orientation vary in a wide range. It has been found that more nodes and collocations are required if the kink is perpendicular to the main clack (consistent of several segments). Therefore two values *n*=8 and *n*=16 have mainly been used in further calculations for perpendicular configurations, while *n*=32 have been used to control accuracy for cracks consistent of moderate number of segments.

3 COMPUTER SIMULATIONS OF CRACK GROWTH

A crack approaching a weak interface (Figure 2a) generates delaminating and sliding zones on the interface ahead of the crack tip (e.g. Parton [8]).

Calculations show that the size of delaminating zone is small compared to the length of the initial crack. Thus if the new crack is initiated at an end of the delaminating zone the SIF at the tip of a considerably small new crack is negative suggesting that the new crack cannot propagate from the ends of delaminating zone. At the same time the length of the sliding zone can be comparable with the length of the initial crack. The new crack can be generated in the direction perpendicular to the interface by the tensile stresses near the end of the sliding zone. When the new crack approaches the next interface a new crack will be generated offset upwards or downwards and so on. Therefore, the process of crack growth can be viewed as a sequence of elementary zigzag steps shown in Figure 1b. The described mechanism of crack propagation is the further development of the concept of "compressional crossing" [3].

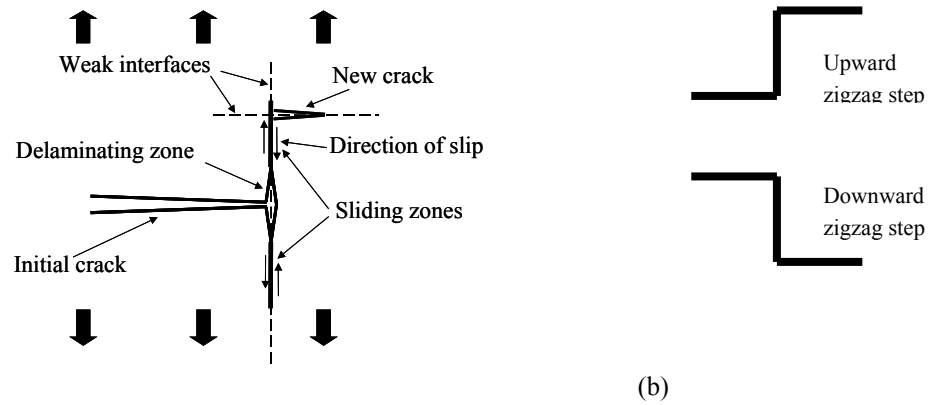

(a) (b)

Figure 1. Crack propagation through the interface: (a) generation of delaminating and sliding zone; (b) an elementary zigzag step of crack propagation each segment having the length equal to 2.

As evident from Figure 1, the crack propagation through the interface is characterised by offsets along the interface. In the case of a system of parallel interfaces the crack path will consist of elementary zigzag steps. The analysis of the SIFs for different sequences of zigzag steps reveals that the trajectories with offsets in the same direction are the most preferable, because they produce the highest SIFs. The trajectories with alternating offset directions are the least preferable. For these two crack paths the dependence of the SIF on the total crack length is investigated. Each segment has unit half-length and the initial crack in both cases consists of two segments. The maximum length of the crack was 10 lengths of the initial crack (L=20). For the case of vertical load applied at infinity the SIF for a crack propagating straight through the material is equal to $K_I=\sigma_0(\pi L/2)^{1/2}$. In the investigated cases the SIFs increase weaker than the square root. The results of calculation of the SIFs (doted curves) and fitting by power functions (solid lines in Figure 2*b, d*) are shown together on Figure 2 with the square root dependence (dash-dot curve) and the dependence $K_I=\sigma_0(\pi\Lambda/2)^{1/2}$, (dash curve) where the effective crack length Λ is the projection of the crack onto horizontal axis.

Several other cases in which the crack path had random offsets have also been investigated. The paths have been specified by random up- or downward zigzag steps. The results of fitting of the calculated SIFs to the power law have shown that the exponent is less than ½ for all analysed cases. This suggests that the power law with the exponent smaller than ½ correctly describes the behaviour of the mode I SIF in random propagation of the crack through the fractured material.

4 CONCLUSIONS

The analysis shows that the preferable crack trajectories are the ones that inclined at an angle to the horizontal direction in which the crack were expected to propagate due to symmetry. One can call this phenomenon the symmetry breaking. The exponent of the power law describing the increase of the mode I SIF with the increasing crack length is close 0.4 as opposite to 1/2 of the conventional crack.

Acknowledgment. The authors acknowledge the financial support from the Australian Research Council through the Discovery Grant`DP0210574 (2002-2004).

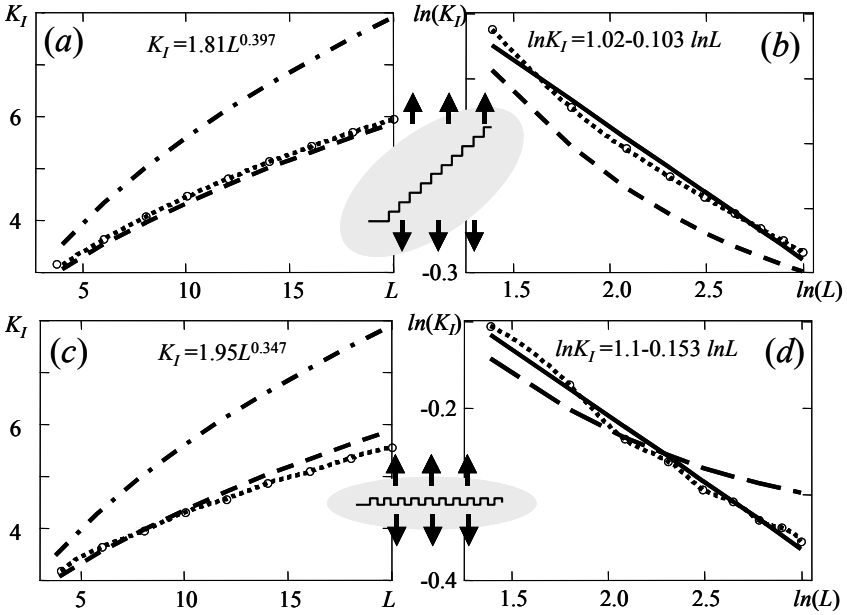

Figure 2. Mode I SIFs vs. total length: the dotted lines show the calculated values; the dash-dotted lines show the case of straight crack with the same total length as the cracks considered; the broken line show the case of straight crack with the total length equal to the projection of the cracks considered; the solid line on log-log graphs show the regression lines.

5 REFERENCES

1. Hoppa, G.V., Tufts, B.R., Greenberg, R. and Geissler, P.E. Formation of cycloidal features on Europa. Science, 285, 1899-1902, 1999.
2. Dyskin, A.V., Estrin, Y., Pasternak, E., Khor, H.C. and Kanel-Belov, A.J. Fracture resistant structures based on topological interlocking with non-planar contacts. *Advanced Engineering Materials*, **5**, No. 3, 116-119, 2003.
3. Renshaw, C.E. and Pollard, D.D. An experimentally verified criterion for propagation across unbounded frictional interface in brittle, linear elastic materials. *Intern. J. Rock Mech. Mining Sci.* 32, 237-249, 1995.
4. McConaughy, D.T. and Engelder, T. Joint interaction with embedded concretions: joint loading configurations inferred from propagation paths. *J. Structur. Geology* 21, 1637-1652 1999.
5. Savruk, M. P. Two-Dimensional Problems of Elasticity for Body with Cracks, Naukova Dumka, Kiev, 1981.
6. Erdogan F. and G.D. Gupta. On the numerical solution of singular integral equations, *Quart. Appl. Math*. 29 525-534, 1972.
7. Murakami, Y. *Stress Intensity Factors Handbook 1*, Pergamon Press, Oxford, 1987.
8. Parton, V.Z., *Fracture Mechanics. From Theory to Practice*. Gordon and Breach Science Publishers, Philadelphia, 1992.